Article

Reactivity of a Unique Si(I)−Si(I)-Based η^2-Bis(silylene) Iron Complex

Zhiyuan He,[#] Lingyu Liu,[#] Felix J. de Zwart, Xiaolian Xue, Andreas W. Ehlers, KaKing Yan, Serhiy Demeshko, Jarl Ivar van der Vlugt,* Bas de Bruin,* and Jeremy Krogman*

Cite This: *Inorg. Chem.* 2022, 61, 11725−11733

Read Online

ACCESS | Metrics & More | Article Recommendations | SI Supporting Information

ABSTRACT: In this paper, we report the synthesis of a unique silicon(I)-based metalla-disilirane and report on its reactivity toward TMS-azide and benzophenone. Metal complexes containing disilylenes ((bis)silylenes with a Si−Si bond) are known, but direct ligation of the Si(I) centers to transition metals always generated dinuclear species. To overcome this problem, we targeted the formation of a mononuclear iron(0)−silicon(I)-based disilylene complex via templated synthesis, starting with ligation of two Si(II) centers to iron(II), followed by a two-step reduction. The DFT structure of the resulting η^2-disilylene-iron complex reveals metal-to-silicon π-back donation and a delocalized three-center−two-electron (3c−2e) aromatic system. The Si(I)−Si(I) bond displays unusual but well-defined reactivity. With TMS-azide, both the initial azide adduct and the follow-up four-membered nitrene complex could be isolated. Reaction with benzophenone led to selective 1,4-addition into the Si−Si bond. This work reveals that selective reactions of Si(I)−Si(I) bonds are made possible by metal ligation.
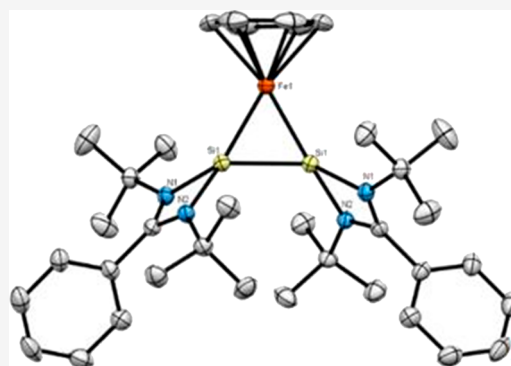
INTRODUCTION

Transition metal silylene complexes (Scheme 1a) have attracted significant interest as they have shown interesting (electronic) structures and reactivity, giving rise to synthetic and catalytic applications that differ significantly from transition metal carbene complexes.[1] Several variants of transition metal silylene complexes have been reported, varying in the oxidation state of the silicon atom and the types of

Scheme 1. (a) Selection of Different Monosilylenes; (b) Difference between "Disilylene" and "Spacer-Separated Bis(silylene)" and Examples of Metal Complexes of the Latter

a. Selected Structures of Silylene Complexes and Their Lewis Base Adducts

Silylene complex | N-heterocyclic silylene complex | Lewis base adduct of a silylene complex | Lewis base adduct of a silylene complex

b. "Disilylene" and "spacer separated bis(silylene)" metal complexes

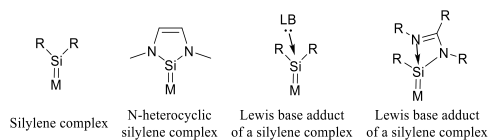"disilylenes" | "spacer-separated bis(silylenes)"

substituents, and among those variants, *N*-heterocyclic silylenes have been studied most extensively.[2]

Two types of the general class of bis(silylene) compounds have been reported: (1) "bis(silylenes) with a direct Si−Si bond", wherein the two divalent silicon atoms are adjacent to each other and are connected by a central Si−Si bond (like others in the field,[3] we term these "disilylenes"); (2) "spacer-separated bis(silylenes)", with the two divalent silicon atoms separated by a spacer.[4] Driess and co-workers recently reported a ferrocene-separated bis(silylene) acting as a bidentate ligand in catalytically active mono- and dicobalt complexes (Scheme 1b).[4e]

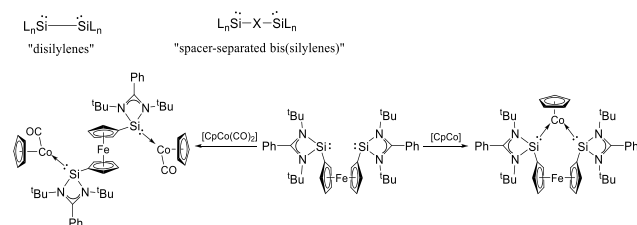We consider "disilylenes" to be particularly interesting due to the potential reactivity associated with their Si−Si bond. Compound **I**, with each Si center bearing an amidinate ligand (Scheme 2), was synthesized by Roesky and co-workers,[5] while Jones *et al.* reported a bulkier derivative thereof.[6] Additionally, "disilylenes" that are stabilized by an *N*-heterocyclic carbene (NHC) or an intramolecular phosphine are also reported.[4a,7] Targeting the synthesis of η^2-coordinated Si(I)-based "disilylene" complexes seems particularly useful because the altered electronic structure and the lability of the Si−Si bond induced

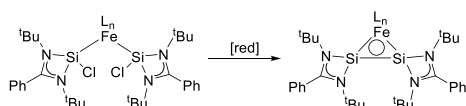**Scheme 2. (a) Reported Di- and Multinuclear Disilylene Transition Metal Complexes; (b) Synthesis and Reactivity of a Mononuclear η^2-Disilylene Iron Complex (This Work)**

a. Known Metal Complexes from Coordination to Si(I)-based disilylene I
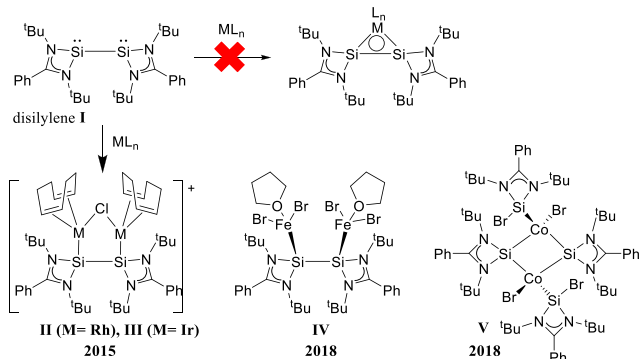
b. This work: η^2-disilylene Complex Formation by Synthesis-at-the-metal.

by η^2-coordination are expected to give rise to unique reactivity.

Thus far, the reported reactivity of these platforms predominantly involves the Si-centered lone pairs rather than the Si—Si σ-bond. For example, So *et al.* reported the formation of the bimetallic disilylene Rh and Ir complexes **II** and **III** (Scheme 2a).[8] Also, the dinuclear iron(II)bromide complex **IV** is formed cleanly, but the Si—Si bond is cleaved by cobalt(II)bromide to form dinuclear cobalt(bromosilylene)-(silyl) complex **V**.[9] To the best of our knowledge, no mononuclear metal adducts of ligand **I** are reported to date.

To achieve η^2-coordination of **I** to a mononuclear transition metal complex, we decided to explore the reductive coupling of two Si(II)-chlorides in the coordination sphere of a metal center (Scheme 2b). We herein describe iron complex **3** as the first η^2-disilylene complex prepared by this protocol (Scheme 3). This species has an unusual electronic structure, with the

Scheme 3. Synthetic Procedure for the Preparation of Complex 3
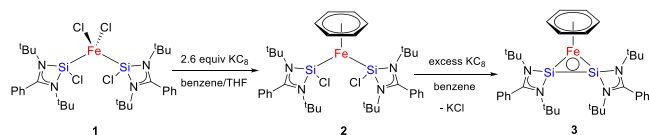
Si—Si bond acting as a π-acceptor moiety, while the three-membered Fe—Si—Si ring shows 2π-aromaticity. It also displays selective Si—Si bond-centered reactivity toward azide activation and ketone addition, giving access to new "spacer-separated bis(silylenes)".

■ RESULTS AND DISCUSSION

Synthesis of 3. The amidinate-stabilized silylene iron-halide precursor **1**, synthesized from Fe{N(SiMe$_3$)$_2$}$_2$ using a literature procedure,[10] was characterized with zero-field ^{57}Fe Mössbauer spectroscopy (Figure 1). The isomer shift δ (0.61 m/s) and the quadrupole splitting ΔE_Q (2.81 mm/s) are in agreement with a four-coordinated Fe(II) center.[11] Iron-
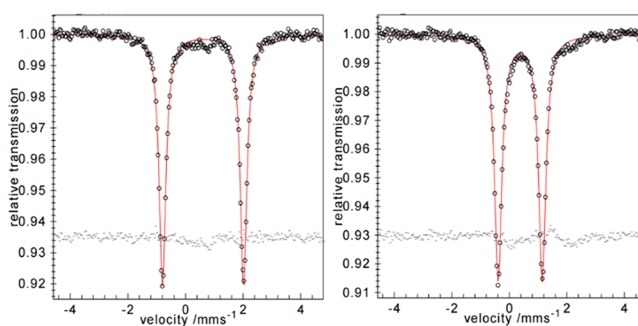
Figure 1. Mössbauer spectra of compounds **1** (left) and **2** (right) at 80 K.

centered reduction of this well-defined Fe(II) species with a slight excess of KC$_8$ in a benzene-THF mixture (1:1 v/v%) generated bis-silylene compound **2**, featuring an η^6-benzene fragment bound to Fe(0).

The ^{1}H NMR spectrum of diamagnetic **2** in deuterated benzene exhibits a chemical shift for the η^6-benzene fragment at δ 5.15 ppm, which is similar to that seen for the previously reported zero-valent iron complex [(SiFcSi)Fe-η^6(C$_6$H$_6$)] bearing a ferrocene-bridged bis(silylene) ligand (δ 5.16 ppm).[12] The ^{29}Si NMR spectrum of **2** exhibits two sharp singlets at δ 45.12 and 42.45 ppm (suggesting chemically inequivalent Si centers), which are close to the reported chemical shift (δ 43.10 ppm) for an *N*-heterocyclic silylene iron(0) complex.[13] Species **2** was also examined using zero-field ^{57}Fe Mössbauer spectroscopy to confirm the oxidation state of Fe (Figure 1). Indeed, both the isomer shift δ (0.38 m/s) and quadrupole splitting ΔE_Q (1.53 mm/s) support reduction to Fe(0).[14]

Single crystals of **2** that were obtained from pentane at −30 °C proved suitable for crystallographic analysis by X-ray diffraction at room temperature; loss of crystallinity was observed at 150 K. The molecular structure (Figure 2) shows
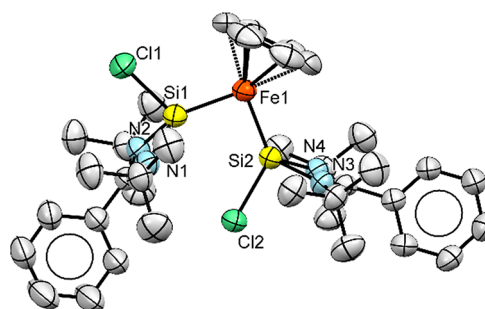
Figure 2. Molecular structure of **2** with thermal ellipsoids drawn at 30% probability. Hydrogen atoms are omitted for clarity. Selected bond lengths (Å) and angles (°): Si1—Fe1, 2.162(2); Si2—Fe1, 2.148(1); Si1—N1, 1.860(5); Si1—N2, 1.866(5); Si1—Si2, 3.100(2); Si1—Fe1—Si2, 91.99(6).

two different orientations for the Si—Cl bonds with respect to the Fe(η^6-benzene) fragment (one "up" and one "down"), which explains the presence of two chemically inequivalent Si nuclei in the ^{29}Si NMR spectrum. The Si—Fe—Si angle is nearly 90° (91.99°), and the intramolecular Si1···Si2 distance is 3.100(2) Å. The Si—Fe1 bond lengths are 2.162(2) Å (Si1) and 2.148(1) Å (Si2), which are significantly shorter than the corresponding bond lengths in precursor **1** (∼2.445 Å) and slightly shorter than those found in the zero-valent iron silylene

complexes ([(NHSi)Fe(dmpe)$_2$] (2.184(2) Å) and Fe(0)-[SiNSi] (2.164(15) and 2.170(13) Å)).[15]

Further reduction of this zero-valent Fe species **2** by an excess of KC$_8$ at room temperature yielded the three-membered metallacyclic complex **3**, featuring a direct Si–Si bond (Scheme 3). This reaction was also monitored using ^{1}H NMR spectroscopy, revealing quantitative conversion (see also Figure S26). The complex was characterized by multinuclear NMR spectroscopy (^{1}H, ^{13}C, and [29]Si). The ^{1}H NMR signal of the Fe-coordinated η^6-benzene shifts from δ 5.15 ppm in **2** to δ 5.34 ppm in **3**. The ^{29}Si NMR spectrum of **3** contains only one singlet at δ 34.49 ppm, indicating formation of a symmetric molecule.

Dark red single crystals of **3** were collected after storing a pentane solution at −30 °C for 1 month. Compound **3** crystallizes in the monoclinic space group C_2/c, which is in line with the high degree of symmetry observed in the ^{1}H NMR spectrum. The Si(I)–Fe–Si(I) three-membered heterocycle forms an equilateral triangle with interatomic distances of 2.217(6) Å (Figure 3); for the Si–Si bond, this value falls in
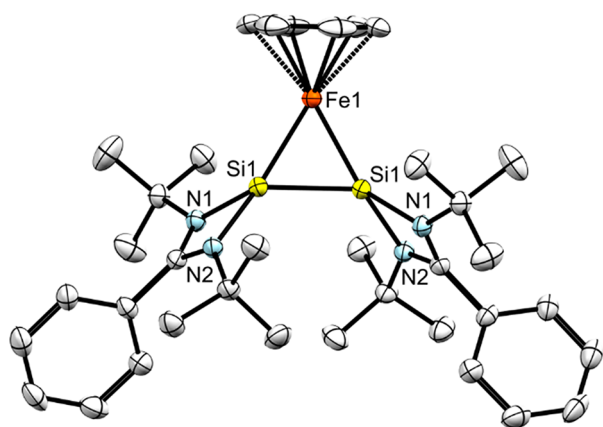

Figure 3. Molecular structure of **3** with thermal ellipsoids drawn at 50% probability. Hydrogen atoms are omitted for clarity. Selected bond lengths (Å) and angles (°): Si1–Si1 and Si1–Fe1, 2.217(6); Si1–N1, 1.865(2); Si1–N2, 1.887(2); Si1–Fe1–Si1, 59.99; Fe1–Si1–Si1, 60.00.

the range observed for Si=Si double bonds (2.120−2.250 Å).[16] The isosceles Si–B–Si disilaborirane compound reported by Roesky and co-workers shows a Si–Si bond length of 2.188(5) Å,[17] while the equilateral triangular (di-*t*-butyl(methyl)silyl)bis(tri-*t*-butylsilyl)cyclotrisilenylium cation has an average Si–Si bond length of 2.217(3) Å.[16]

Electronic Structure of 3. Given the unprecedented nature of the ferracyclic motif found in this species, the bonding of the Si(I)–Si(I) fragment to iron(0) was theoretically investigated at the TZ2P/OPBE[18] level of theory using energy decomposition analysis (EDA).[19] The lowest energy structure with C_2 symmetry is analogous to that derived from X-ray diffraction. To facilitate the EDA analysis (for symmetry reasons), the bonding of the disilylene moiety to iron has been analyzed using a C_{2v} optimized structure, which is only 4.4 kcal·mol^{-1} higher in energy. This small energy difference is consistent with the dynamic behavior observed in solution-state NMR spectroscopy, resulting in a single signal for the ^{t}Bu substituents at nitrogen.

The Fe(η^6-benzene) fragment has been computed in the singlet state (Fe(0)-d^8). It has a two-electron occupied d$_{xz}$

orbital (perpendicular to the Si–Fe–Si plane) and an empty d$_{yz}$ orbital. The electronic structure of the Si(I)–Si(I) fragment is best described as having a Si–Si single bond with a lone pair on each silicon atom and an empty π-orbital perpendicular to that plane (Figure S31). The symmetry-adapted linear combinations of the two lone pairs on silicon donate electron density toward the Fe(η^6-benzene) fragment, forming two (delocalized) σ-bonds of −30.3 kcal·mol^{-1} (A1) and −74.4 kcal·mol^{-1} (B1). The iron itself donates electron density back from the occupied d$_{xz}$ orbital into an empty π-orbital formed by the two Si p$_z$ orbitals (B2: −67.8 kcal·mol^{-1}), giving rise to considerable π-backbonding (Figure 4).
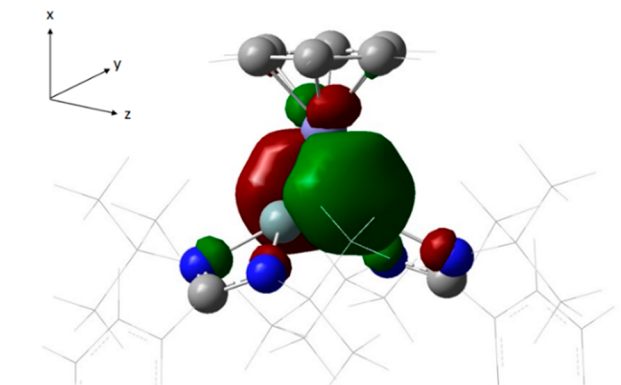

Figure 4. Graphical representation of the Fe-to-(Si–Si) π-back donation in **3**.

To probe the resulting orbital (which is delocalized over the Si–Fe–Si three-membered ring) for aromaticity, we employed the nucleus-independent chemical shift (NICS(0/1)) approach at the B3LYP/6-11+G(d,p) level (negative value of the isotropic magnetic shielding at the center of the Fe–Si–Si three-membered ring and 1 Å perpendicularly above and below, respectively). These are found to be −47.8 and −21.4 ppm, respectively, corroborating the magnetic aromaticity. For comparison, the NICS(0/1) values at the center of the benzene ring in **3** are calculated to be −42.8 and −18.4 ppm. Similar values have been reported for other metallacycles.[20] A more refined method by Stanger[21] following the out-of-plane component to the shielding tensor along a trajectory orthogonal to the plane of the ring (NICS$_{zz}$) has been used by Roesky *et al.* to assign 2π-aromaticity to their disilaborirane species.[17] However, instead of showing the typical off-center minimum for 2π-aromatic systems, the NICS scan of **3** shows a steady and continuous increase to less negative NICS$_{zz}$ values over a value of 3 Å (see Figure S33), which may be caused by anisotropy of the metal center at the ring and/or by σ-aromaticity.[17,19,22]

Therefore, we resorted to the canonical molecular orbital (CMO) analysis of the NICS(0), which separates the total shieldings into contributions from canonical molecular orbitals.[23] Indeed, there is a sizable contribution of −13.8 ppm from the Fe d$_{xy}$ orbital (HOMO−5, see Figure S32), which is part of the σ-framework. More importantly, the major contribution of −16.6 ppm originates from the delocalized π-orbital shown in Figure 4, substantiating the 2π-aromaticity of the Si$_2$Fe three-membered ring in complex **3**.

Reactivity of 3. The unligated Si(I)-based disilylene species **I** shows stoichiometry-dependent reactivity toward trimethylsilyl azide, forming either a silaazatriene or a silaimine

product.[24,25] Roesky and co-workers described ring opening of their disilaborirane species **VI** with TMSN₃, forming a 1-aza-2,3-disila-4-boretidine derivative (Scheme 4).[17] We observed

Scheme 4. Synthetic Scheme for the Preparation of Azide Adduct 4 and Final Product 5 upon Reaction of 3 with Trimethylsilyl Azide
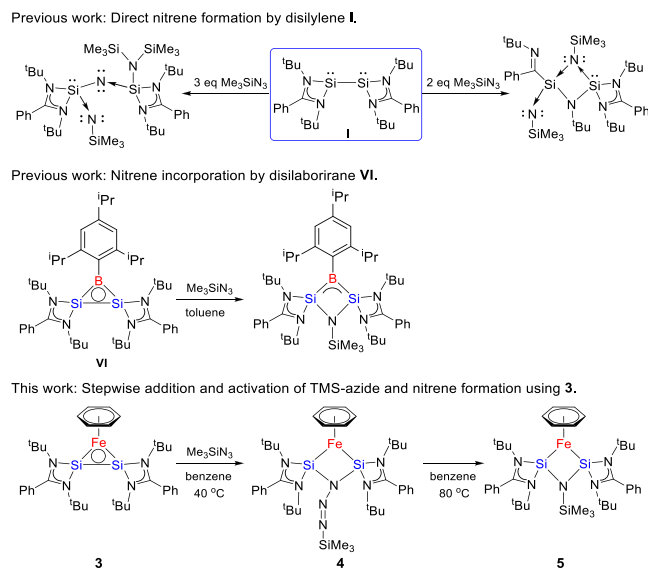
selective conversion of **3** with 1 equiv of TMSN₃ to give the unique azide adduct **4** after 1 h at 40 °C in benzene solution. This species was obtained as a single crystalline material by recrystallization from pentane at −30 °C. The molecular structure, as determined by X-ray diffraction, is displayed in Figure 5. It contains a planar four-membered Si1−Fe1−Si2−N5 heterocycle resulting from the insertion of the azide terminal N-atom in the Si−Si bond, with Fe−Si−N5 angles of roughly 100°. The two Si−Fe distances are slightly different, Si1/2−Fe1 (2.1687(6) and 2.1746(7) Å). The intramolecular Si⋯Si distance is long at 2.504(8) Å.

Prolonged heating of a mixture of **3** with TMSN₃ or isolated **4** at 80 °C generated the follow-up trimethylsilylnitrene complex **5** as the major product, together with small amounts of intermediate **4** (see Figure S17). Single crystals of **5**, obtained by recrystallization from benzene at room temperature, were analyzed by X-ray diffraction (Figure 5).

Compound **5** also shows a planar four-membered Si1−Fe1−Si2−N5 heterocycle with Fe−Si−N5 angles of 103(1)° but with a different substitution pattern at N5, i.e., only a TMS group resulting from the insertion of trimethylsilylnitrene in the Si−Si bond. The two Si−Fe distances are nearly identical, Si1/2−Fe1 (2.174(2) and 2.177(2) Å), and so are the Si1/2−N5 (1.770(5) and 1.767(4) Å) bond lengths. The Si−Fe σ-bonds are on average 0.2547 Å longer than the Si−B distance in the N-insertion product obtained from disilaborirane,[18] while the Si−N5 bond length is similar. The intramolecular Si⋯Si distance (2.412(2) Å) in **5** is shortened relative to that in **4**. Apart from the X-ray crystallographic analysis, reaction monitoring and product identification have also been achieved using NMR spectroscopy. The ¹H NMR signal of the Fe-bound η^6-benzene fragment shifts from δ 5.34 ppm (**3**) to δ 5.26 ppm (**4**) and 5.12 ppm (**5**), and the trimethylsilyl group in azide adduct **4** appears at δ 0.47 ppm (for **5**, δ 0.39 ppm) compared to −0.08 ppm for TMSN₃. In ²⁹Si NMR, the N*Si*N signals for both **4** and **5** are strongly upfield-shifted ($\Delta\delta \sim 27$ ppm) with respect to **3** (**4**: δ 7.05 ppm; **5**: δ 7.42 ppm), in line with the rupture of the Si−Si bond, which also disrupts the 2π-aromaticity and leads to loss of ring current. The $Si(CH_3)_3$ signal appears at δ 15.41 ppm for **4** and at −20.71 ppm for **5**.

To understand the observed two-step reaction between **3** and trimethylsilylazide, we used DFT calculations to explore the reaction mechanism. The initial step involves the nucleophilic attack of the azide onto one of the Si centers, which results in induced nucleophilic character at the second Si center that subsequently attacks back onto the azide in **TS1** (Figure 6). As a result, this insertion can be considered to involve induced FLP reactivity. The energy barrier to afford **Int1** (15.4 kcal·mol⁻¹) is consistent with the experimentally determined barrier (15.1 kcal·mol⁻¹) for formation of **4** (Arrhenius plot, Figure 5). After forming this symmetric azide adduct, the energy barrier for the subsequent dinitrogen release (29.4 kcal·mol⁻¹) is high enough to rationalize the successful isolation of **4**. Finally, a Staudinger pathway, involving four-membered ring transition state **TS3**, releases dinitrogen from **4** to afford product **5** (−110 kcal·mol⁻¹).

The ambivalent reactivity of the Si(I) centers in the Si−Si bond of **3**, able to act either as nucleophile or electrophile, was also apparent during the conversion of species **3** conversion with benzophenone. Disilylene **I** was previously reported to react with benzophenone to furnish selective C−O cleavage with formation of a cyclodisiloxane (Scheme 5).[26] Strikingly

Figure 5. X-ray crystal structures of **4** (left) and **5** (right) with thermal ellipsoids drawn at 50% probability. Hydrogen atoms are omitted for clarity. Selected bond lengths (Å) and angles (°) of **4**: Si1⋯Si2, 2.5040 (8); Si1−Fe1, 2.1687(6); Si2−Fe1, 2.1746(7); Si1−N5, 1.784(2); Si2−N5, 1.791(2); Si1−Fe1−Si1, 70.41(2); Fe1−Si1−N5, 100.57(6); Fe1−Si2−N5, 100.11(6); Si1−N5−Si2, 88.91(8); **5**: Si1⋯Si2, 2.412(2); Si1−Fe1, 2.174(2); Si2−Fe1, 2.177(2); Si1−N5, 1.770(5); Si2−N5, 1.767(4); Si1−Fe1−Si1, 67.33(6); Fe1−Si1−N5, 103.30(1); Fe1−Si2−N5, 103.30(1); Si1−N5−Si2, 86.00(2).
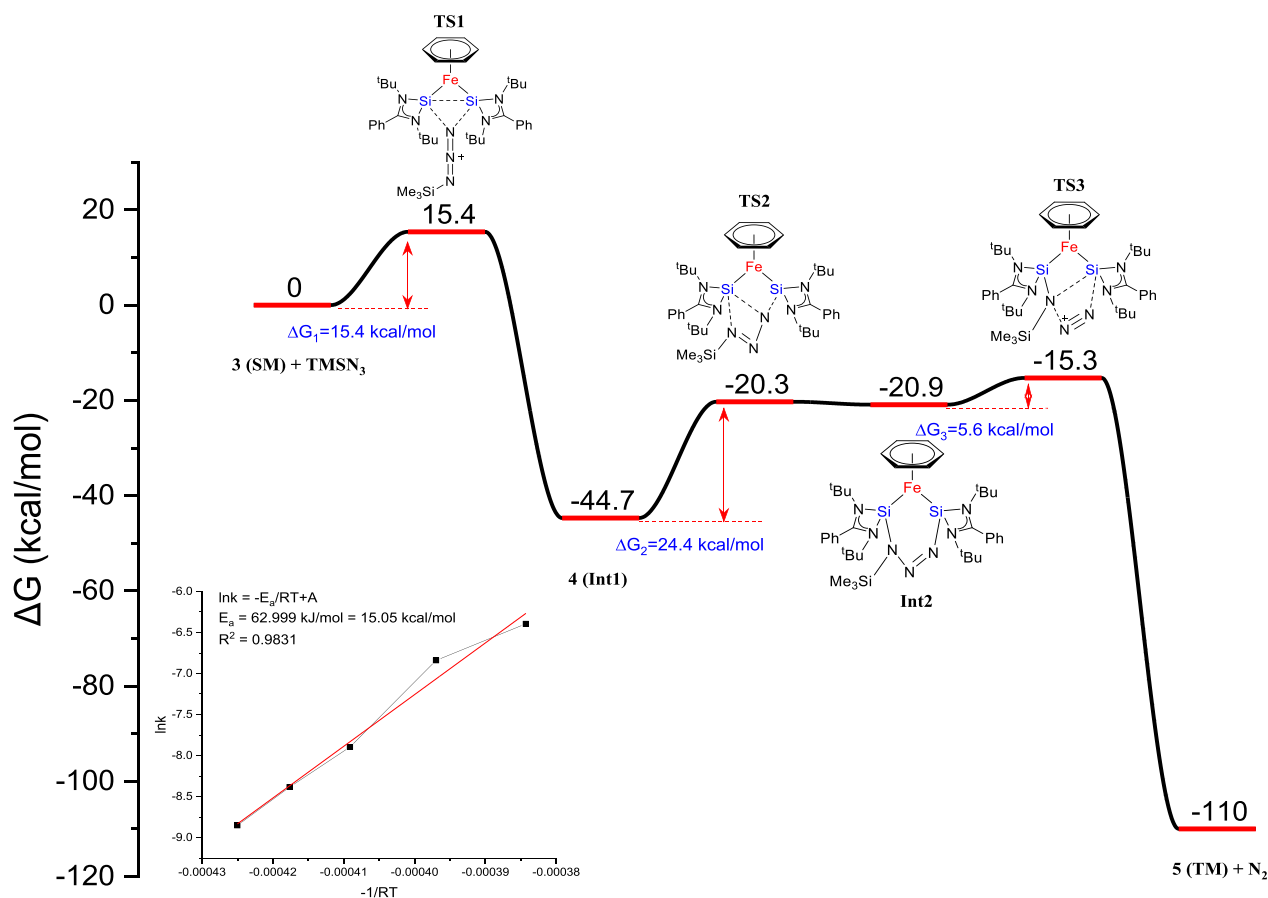
Figure 6. Computed free energy profile for nitrene formation from trimethylsilyl azide and complex **3** (B3LYP-TZVP and def2-TZVP). Transient bonds in transition states are drawn as dashed lines. The inset shows the Arrhenius plot for the consumption of **3** (for details, see the Supporting Information).

Scheme 5. Synthetic Scheme for the Preparation of 6
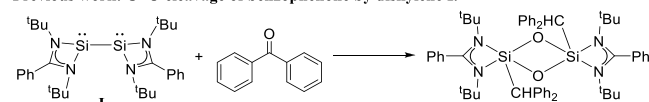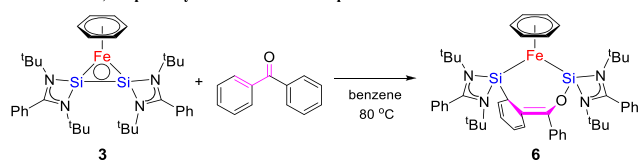
different reactivity was observed when complex **3**, featuring a "protected" Si−Si bond, was exposed to benzophenone for 1 h at 80 °C. Selective formation of seven-membered ring product **6** was obtained via a formal 1,4-addition of benzophenone, displaying strongly attenuated and controlled reactivity of the Si−Si fragment in complex **3**. Complex **6** was characterized in the solid state using single-crystal X-ray diffraction (Figure 7). The structure consists of a nonplanar seven-membered O−Si− Fe−Si−C−C−C ring (angle between the planes O1−C37− C44−C49 and O1−Si1−Fe1−Si2 is 7.20°). The C37−C44 bond length (1.348(5) Å) lies in between that of a typical single carbon bond and a double carbon bond (1.510−1.317 Å).[27] The Si−Fe−Si angle (∠88.21(4)°) is larger than in species **4** and **5** because of increased steric hindrance. One of the phenyl rings has undergone *ortho*-silylation, concomitant
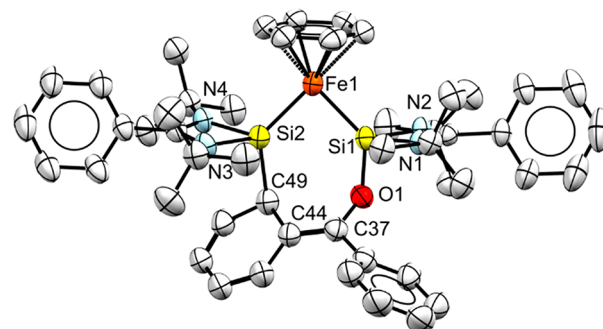
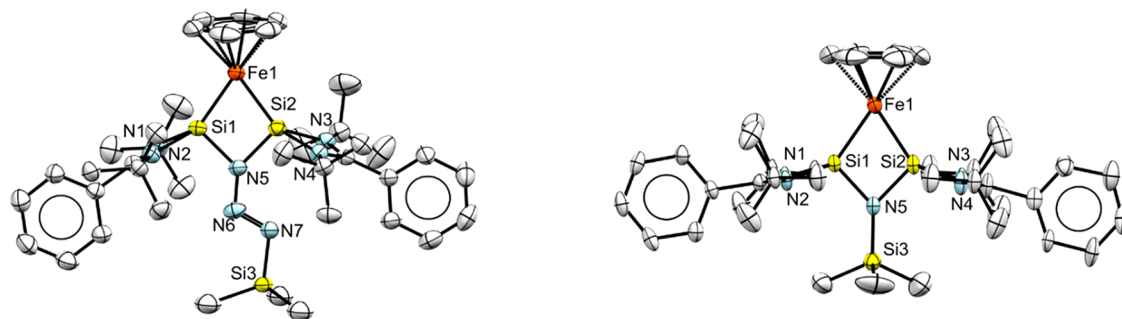**Figure 7.** X-ray crystal structure of **6** with thermal ellipsoids drawn at 50% probability. Hydrogen atoms are omitted for clarity. Selected bond lengths (Å) and angles (°) of **6**: Si1···Si2, 3.101(1); Si1−Fe1, 2.146(9); Si2−Fe1, 2.179(9); Si1−O1, 1.688(2); O1−C37, 1.384(3); C37−C44, 1.348(5); C44−C49, 1.503(5); C49−Si2, 1.983(4); Si1− Fe1−Si1, 88.21(4).

with ring de-aromatization and formation of an enolate-type fragment bound via the oxygen to the second Si center. As a result, overall 1,4-addition of benzophenone has occurred, with no sign of the 1,2-C,O addition product. The ^{1}H NMR signal for the η^6-benzene fragment shifts from δ 5.34 ppm (**3**) to δ 5.07 ppm (**6**). The C−H hydrogen at the *ortho*-silylated position resonates at around δ 6.99 ppm according to 2D-COSY NMR spectroscopy, while the other four hydrogens of the de-aromatized ring appear in the range of 4.90−6.20 ppm. The ^{29}Si NMR spectrum of **6** exhibits two sharp singlets at δ

65.57 and δ 33.66 ppm, in accordance with the two different bonding features.

CONCLUSIONS

In summary, we have developed an efficient method to synthesize the first example of a mononuclear transition metal complex bearing a ligated Si(I)−Si(I) disilylene fragment, ferracyclic η^2-disilylene complex **3**. The electronic structure of this species shows that the Si−Si fragment acts as a four-electron σ-donor to iron, while significant π-back donation from the iron(0) center to the silicon atoms of the disilylene moiety leads to further stabilization of the overall structure. Complex **3** shows well-defined nucleophile-induced FLP reactivity toward TMS-azide and benzophenone, leading to Si−Si bond cleavage by addition of the reagents to the Si_2 fragment, generating unexpected four- and seven-membered ring structures. Expanding this unique reactivity to other small molecules is currently being explored within our groups.

EXPERIMENTAL SECTION

Materials and Methods. Unless otherwise stated, all manipulations were performed under a nitrogen atmosphere using Schlenk techniques or in a Vigor glovebox maintained at or below 1 ppm of O_2 and H_2O. All new metal complexes were prepared and handled in the glovebox under a N_2 atmosphere. Anhydrous $FeCl_2$ (98%) was purchased from Strem Chemicals. $PhC(N^tBu)_2SiHCl_2$,[28] LiN-$(SiMe_3)_2(Et_2O)$,[28] $Fe(N(SiMe_3)_2)_2$,[29] and complex **1** ($FeCl_2\{PhC-(N^tBu)_2SiCl\}_2$)[10] were synthesized according to reported procedures. Other reagents were purchased from J&K Chemical and SCRC. Glassware was dried at 150 °C overnight. Celite and molecular sieves were dried at 200 °C under vacuum. Benzene, pentane, hexanes, and diethyl ether were degassed with nitrogen, dried over activated molecular sieves, and kept over 4 Å molecular sieves in a N_2-filled glovebox. NMR data were recorded either on a Bruker 400 or a 500 MHz spectrometer and were internally referenced to residual proton solvent signals in C_6D_6 (7.16 ppm). Data for ${}^1H$ NMR are reported as follows: chemical shift (δ ppm) and multiplicity (s = singlet, d = doublet, t = triplet, m = multiplet, br = broad). IR data were recorded on a Thermo Scientific Nicolet iS5 FTIR, and signal strength is represented as follows: VS = very strong, W = weak, S = strong, VW = very weak, m = middle, w = wide. The UV−Vis spectra were recorded using a StellarNet BLACK Comet C-SR diode array miniature spectrophotometer connected to deuterium and halogen lamp by optical fiber using 1 cm matched quartz cuvettes at room temperature. Elemental analysis was performed by the Analytical Laboratory of Shanghai Institute of Organic Chemistry (CAS).

X-ray Crystallography. Crystals were coated with Paratone-N oil and mounted on a Bruker D8 Venture diffractometer equipped with an APEX-II CCD diffractometer. The crystal was kept at 150 K during data collection. Using Olex2,[30] the structure was solved with the ShelXT[31] structure solution program using Intrinsic Phasing and refined with the XL[32] refinement package using least squares minimization. CCDC 2157512−2157516 contain the supplementary crystallographic data for this paper. These data can be obtained free of charge from The Cambridge Crystallographic Data Centre via www.ccdc.cam.ac.uk/data_request/cif.

Mössbauer Spectroscopy. Mössbauer spectra were recorded with a ${}^{57}Co$ source in a Rh matrix using an alternating constant acceleration Wissel Mössbauer spectrometer operated in transmission mode and equipped with a Janis closed-cycle helium cryostat. Isomer shifts are given relative to the iron metal at ambient temperature. Simulation of the experimental data was performed with the Mfit program (developed by Dr. E. Bill, Max-Planck Institute for Chemical Energy Conversion, Mülheim/Ruhr, Germany) using Lorentzian line doublets.

Computational Details. Geometries were fully optimized as minima or transition states using the Turbomole program package,[33]

coupled to the PQS Baker optimizer[34] via the BOpt package.[35] We used unrestricted ri-DFT-D3 calculations at the B3LYP level,[36] in combination with the def2-TZVP basis set[37] and a small (m4) grid size. Grimme's dispersion corrections[38] (version 3, disp3, "zero damping") were used to include van der Waals interactions. The energy decomposition analysis (EDA)[19] was performed on the TZ2P/OPBE[18] optimized geometry constrained to C_{2v} symmetry (+3.9 kcal·mol^{-1}). The nucleus-independent chemical shift (NICS)[39] was used as a diagnostic probe for quantitative measure for aromaticity at the B3LYP/6-11+G(d,p) level.[40,41] For further details, see the Supporting Information.

{PhC(N^tBu)_2SiCl}_2Fe(C_6H_6) (2). A solution of **1** (110 mg, 0.153 mmol) in benzene (5 mL) was added dropwise to a solution of KC_8 (53.7 mg, 0.398 mmol) in THF (5 mL) in a vial while stirring. The color of the reaction mixture turned from yellow to dark red-brown. After stirring for 12 h, volatile materials were removed under vacuum and compound **2** was extracted with pentane solution. The solid was crystallized in pentane solution in a −30 °C freezer for 2 days, and only crystalline material was used for subsequent reactions (yield: 40 mg, 40%). ${}^1H$ NMR (500 MHz, benzene-d_6, ppm) δ 8.04 (m, 1H, Ar-H), 7.26 (d, 1H, Ar-H), 7.09 (d, 1H, Ar-H), 7.00−6.9 (m, 6H, Ar-H), 6.86 (t, 1H, Ar-H), 5.15 (s, 6H, benzene-H), 1.52 (s, 18H, N^tBu-H), 1.31 (s, 18H, N^tBu-H). ${}^{13}C$ NMR (126 MHz, benzene-d_6, ppm) δ 171.84 (NCN), 170.75 (NCN), 132.55, 132.44, 129.80, 129.70, 129.47, 129.24, 129.02, 128.84, 128.55, 127.63, 127.36 (132.55−127.36: Ph), 80.23 (Fe-benzene), 54.24 (CMe_3), 53.64 (CMe_3), 31.86 (CH_3), 31.39 (CH_3). ${}^{29}Si$ NMR (99 MHz, benzene-d_6, ppm) δ 45.12, 42.45. UV−Vis (THF, λ (nm) (ε, $M^{-1}\cdot cm^{-1}$)): 410 (1604). IR-ATR (cm^{-1}): 3059 (VW), 2970 (w), 2928 (VW), 2868 (VW), 1640 (VW), 1577 (VW), 1519 (VW), 1472 (m), 1443 (m), 1415.63 (S), 1389 (S), 1361 (S), 1272 (m), 1203 (S), 1085 (m), 1022 (m), 972 (VW), 926 (W), 882 (W), 789 (W), 753 (S), 726 (W), 708 (S), 636 (m), 617 (S). Anal. calcd for $C_{36}H_{52}Cl_2FeN_4Si_2$: C, 59.74; H, 7.24; N, 7.74. Found: C, 57.43; H, 7.29; N, 7.77. Note: Due to the formation of silicon carbide, the carbon values in the elemental analyses were consistently too low for all the disilylene Fe compounds reported in this paper.

{PhC(N^tBu)_2Si}_2Fe(C_6H_6) (3). A solution of **2** (37 mg, 0.051 mmol) in benzene (10 mL) was added dropwise to KC_8 (42 mg, 0.311 mmol) in a vial with stirring. About 20 mg of KC_8 was added every 3 h until all material was converted to $\{PhC(N^tBu)_2Si\}_2Fe(C_6H_6)$, which can be determined by ${}^1H$ NMR monitoring. The color of the reaction mixture turned from red-brown to black. Compound **3** (yield: 29 mg, 89.3%) was collected by removing solvents and volatile materials under vacuum. The solid was stored in pentane solution in a −30 °C freezer for 1 month to give X-ray quality crystals. ${}^1H$ NMR (500 MHz, benzene-d_6) δ 7.14 (m, 2H, Ar-H), 7.00−6.9 (m, 6H, Ar-H), 6.80 (td, 2H, Ar-H), 5.34 (s, 6H, benzene-H), 1.47 (s, 36H, N^tBu-H). ${}^{13}C$ NMR (126 MHz, benzene-d_6, ppm) δ 162.70 (NCN), 135.72, 129.91, 128.98, 128.93, 127.77, 127.56 (135.72−127.56: Ph), 76.74 (Fe-benzene), 54.62 (CMe_3), 32.78 (CH_3). ${}^{29}Si$ NMR (99 MHz, benzene-d_6, ppm) δ 34.49. UV−Vis (THF, λ (nm) (ε, $M^{-1}\cdot cm^{-1}$)): 390 (4280). IR-ATR (cm^{-1}): 3047 (W), 2961 (m), 2922 (m), 2855 (W), 1957 (VW), 1598 (W), 1442 (VW), 1403 (W), 1387 (VS), 1356 (S), 1266 (m), 1203 (S), 1071 (m), 1029 (W), 965 (W), 925 (W), 889 (VW), 836 (VW), 791 (W), 752 (S), 704 (VS), 654 (VW), 610 (m), 560 (VW). Anal. calcd for $C_{36}H_{52}FeN_4Si_2$: C, 66.23; H, 8.03; N, 8.58. Found: C, 65.11; H, 8.17; N, 8.57.

{PhC(N^tBu)_2Si}_2Fe(C_6H_6)(N_3SiMe_3) (4). Compound **4**, which is also formed during the formation of species **5** (vide infra), can be obtained as an isolable species upon reaction of **3** with $TMSN_3$ (7.5 μL, 0.153 mmol) for 1 h at 40 °C in benzene solution in a J-Young tube (quantitative conversion). After 40 min of reaction, the solution was evaporated to dryness under vacuum and redissolved in pentane. X-ray quality crystals were grown from a pentane solution stored in a −30 °C freezer. ${}^1H$ NMR (500 MHz, benzene-d_6) δ 7.32 (dt, 2H, Ar-H), 7.22 (m, 1H, Ar-H), 7.11 (m, 2H, Ar-H), 7.04 (t, 2H, Ar-H), 7.00 (t, 2H, Ar-H), 6.97 (d, 1H, Ar-H), 5.26 (s, 6H, benzene-H), 1.33 (s, 36H, N^tBu-H), 0.47 (s, 9H, Si(CH_3)$_3$). ${}^{13}C$ NMR (126 MHz, benzene-d_6, ppm) δ 159.33−127.76 (5 signals; 2 Ph), 76.66 (Fe-

benzene), 53.68 (CMe$_3$), 32.04 (CH$_3$), −0.08 (Si(CH$_3$)$_3$), −1.23 (N$_3$Si(CH$_3$)$_3$). ^{29}Si NMR (99 MHz, benzene-d_6, ppm) δ 15.41, 7.05. UV−Vis (THF, λ (nm) (ε, M^{-1}·cm^{-1})): 485 (2343). IR-ATR (cm^{-1}): 3048 (VW), 2962 (W), 2033 (W), 1523 (VW), 1472 (W), 1422 (S), 1391 (W), 1358 (W), 1274 (W), 1237 (W), 1207 (S), 1148 (m), 1078 (W), 1021 (W), 989 (m), 966 (W), 923 (W), 832 (S), 789 (W), 751 (S), 724 (W), 704 (S), 641 (W), 609 (W). Elemental analysis of this species did not yield satisfactory results, which is attributed to the demonstrated thermal instability of this complex, leading to "decomposition" to form species **5**.

{PhC(N^{t}Bu)$_2$Si}$_2$Fe(C$_6$H$_6$)(NSiMe$_3$) (**5**). TMSN$_3$ (7.5 μL, 0.153 mmol) was added by a pipette to a solution of **3** (36 mg, 0.055 mmol) in a J-Young tube or Schlenk tube while stirring at 80 °C. After heating the reaction mixture for 90 min, the product was isolated (yield: 20.3 mg, 50%) as a purple-red solid by removing all solvents and other volatile materials under vacuum and washing with cold pentane. At shorter reaction times, this product coexists with complex **4** according to NMR spectroscopy. X-ray quality crystals were collected by dissolving the obtained solid in benzene solution and slow evaporation of the solution at room temperature. ^{1}H NMR (500 MHz, benzene-d_6) δ 7.36 (s, 1H, Ar-H), 7.31 (d, 3H, Ar-H), 7.01−6.99 (m, 4H, Ar-H), 6.96 (m, 2H, Ar-H), 5.12 (s, 6H, benzene-H), 1.43 (s, 36H, N^{t}Bu-H), 0.39 (s, 9H, Si(CH$_3$)$_3$). ^{13}C NMR (126 MHz, benzene-d_6, ppm) δ 169.61 (NCN), 133.69, 129.94, 128.47, 127.67 (133.69−127.67: Ph), 75.31 (Fe-benzene), 53.61 (CMe$_3$), 31.75 (CH$_3$), 3.79 (NSi(CH$_3$)$_3$). ^{29}Si NMR (99 MHz, benzene-d_6, ppm) δ 7.42, −20.71. UV−Vis (THF, λ (nm) (ε, M^{-1}·cm^{-1})): 530 (592). IR-ATR (cm^{-1}): 3357 (VW), 2961 (w), 2029 (S), 1597 (W), 1473 (VW), 1419 (S), 1392 (W), 1358 (m), 1237 (W), 1204 (S), 1074 (W), 1019 (S), 924 (VW), 832 (S), 787 (VW), 746 (S), 704 (S), 649 (VW), 641 (VW), 609 (W). Anal. calcd for C$_{39}$H$_{61}$FeN$_5$Si$_3$: C, 63.30; H, 8.31; N, 9.46. Found: C, 60.19; H, 7.99; N, 8.82.

{PhC(NtBu)$_2$Si}$_2$Fe(C$_6$H$_6$)(Ph$_2$CO) (**6**). Benzophenone (437 μL of a 100 mg/10 mL stock solution in benzene) was added dropwise to a solution of **3** (15.6 mg) in benzene (5 mL) in a J-Young tube or Schlenk tube at 80 °C with stirring. Product **6** was isolated as a dark greenish-black solid by washing with cold pentane after removing all solvents and other volatile materials. Yield: 12 mg, 60%. X-ray quality crystals were collected by dissolving the solid in diethyl ether solution and then placing the sample in a −30 °C freezer. ^{1}H NMR (500 MHz, benzene-d_6) δ 8.36 (d, 0.5H, Ar-H), 7.76 (d, 2H, Ar-H), 7.52 (d, 1H, Ar-H), 7.31 (d, 0.5H, Ar-H), 7.25 (t, 2H, Ar-H), 7.06−6.95 (m, 9H, Ar-H), 6.98 (d, 1H, de-ArCH), 6.17 (dd, 1H, de-ArCH), 5.86 (m, 1H, de-ArCH), 5.65 (dd, 1H, de-ArCH), 4.90 (d, 1H, de-ArCH), 5.07 (s, 6H, benzene-H), 1.59/1.45/1.31/0.97 (s, 9H, N^{t}Bu-H). ^{13}C NMR (126 MHz, benzene-d_6, ppm) δ 170.46 (NCN), 167.56 (NCN), 159.33−122.22 (18 signals; 6 C + 18 C; CCCHCHCHCH + C of 3 Ph), 78.46 (Fe-benzene), 53.23 (CMe$_3$), 53.14 (CMe$_3$), 52.67 (CMe$_3$), 52.38 (CMe$_3$), 32.12 (CH$_3$), 32.01 (CH$_3$), 31.15 (CH$_3$), 31.09 (CH$_3$). ^{29}Si NMR (99 MHz, benzene-d_6, ppm) δ 65.57, 33.66. UV−Vis (THF, λ(nm) (ε, M^{-1}·cm^{-1})): 350 (4785), 435 (2782). IR-ATR (cm^{-1}): 3052 (VW), 2965 (W), 2962 (VW). 1647 (VW), 1596 (VW), 1472 (W), 1421 (S), 1390 (m), 1358 (m), 1264 (m), 1204 (S), 1106 (VW), 1072 (W), 1009 (W), 970 (W), 923 (W), 865 (W), 790 (m), 745 (S), 722 (VW), 699 (VS), 607 (S), 544 (S). Anal. calcd for C$_{49}$H$_{62}$FeN$_4$OSi$_2$: C, 70.48; H, 7.48; N, 6.71. Found: C, 65.07; H, 7.09; N, 6.15.

ASSOCIATED CONTENT

Supporting Information

The Supporting Information is available free of charge at https://pubs.acs.org/doi/10.1021/acs.inorgchem.2c01369.

> General information; synthetic procedures of new compounds, including NMR, IR, and UV−Vis spectra; reaction of **3** with TMS-azide followed by NMR; EDA and DFT calculations; single-crystal X-ray data diffraction (PDF)
>
> Computational details (ZIP)

Accession Codes

CCDC 2157512−2157516 contain the supplementary crystallographic data for this paper. These data can be obtained free of charge via www.ccdc.cam.ac.uk/data_request/cif, or by emailing data_request@ccdc.cam.ac.uk, or by contacting The Cambridge Crystallographic Data Centre, 12 Union Road, Cambridge CB2 1EZ, UK; fax: +44 1223 336033.

AUTHOR INFORMATION

Corresponding Authors

Jarl Ivar van der Vlugt − *van't Hoff Institute for Molecular Sciences, University of Amsterdam, 1098 XH Amsterdam, The Netherlands; Institute of Chemistry, Carl von Ossietzky University, 12629 Oldenburg, Germany;* orcid.org/0000-0003-0665-9239; Email: jarl.ivar.van.der.vlugt@uni-oldenburg.de

Bas de Bruin − *van't Hoff Institute for Molecular Sciences, University of Amsterdam, 1098 XH Amsterdam, The Netherlands;* orcid.org/0000-0002-3482-7669; Email: b.debruin@uva.nl

Jeremy Krogman − *School of Physical Science and Technology, ShanghaiTech University, Shanghai 201210, China;* Email: jkrogman@shanghaitech.edu.cn

Authors

Zhiyuan He − *School of Physical Science and Technology, ShanghaiTech University, Shanghai 201210, China; van't Hoff Institute for Molecular Sciences, University of Amsterdam, 1098 XH Amsterdam, The Netherlands*

Lingyu Liu − *School of Physical Science and Technology, ShanghaiTech University, Shanghai 201210, China*

Felix J. de Zwart − *van't Hoff Institute for Molecular Sciences, University of Amsterdam, 1098 XH Amsterdam, The Netherlands;* orcid.org/0000-0002-0981-1120

Xiaolian Xue − *School of Physical Science and Technology, ShanghaiTech University, Shanghai 201210, China*

Andreas W. Ehlers − *van't Hoff Institute for Molecular Sciences, University of Amsterdam, 1098 XH Amsterdam, The Netherlands; Department of Chemistry, University of Johannesburg, Johannesburg ZA-2006, South Africa*

KaKing Yan − *School of Physical Science and Technology, ShanghaiTech University, Shanghai 201210, China;* orcid.org/0000-0001-6963-6099

Serhiy Demeshko − *Department of Chemistry, Georg August University, 37077 Göttingen, Germany*

Complete contact information is available at:
https://pubs.acs.org/10.1021/acs.inorgchem.2c01369

Author Contributions

#Z.H. and L.L. contributed equally to this work. All authors have given approval to the final version of the manuscript.

Notes

The authors declare no competing financial interest.

■ REFERENCES

(1) Blom, B.; Stoelzel, M.; Driess, M. New Vistas in N-Heterocyclic Silylene (NHSi) Transition-Metal Coordination Chemistry: Syntheses, Structures and Reactivity towards Activation of Small Molecules. *Chem. − Eur. J.* **2013**, *19*, 40−62.

(2) Denk, M.; Lennon, R.; Hayashi, R.; West, R.; Belyakov, A. V.; Verne, H. P.; Haaland, A.; Wagner, M.; Metzler, N. Synthesis and Structure of a Stable Silylene. *J. Am. Chem. Soc.* **1994**, *116*, 2691−2692.

(3) (a) Yeong, H. X.; Lau, K. C.; Xi, H. W.; Lim, K. H.; So, C. W. Reactivity of a Disilylene $[\{PhC(NBu^t)_2\}Si]_2$ toward Bromine: Synthesis and Characterization of a Stable Monomeric Bromosilylene. *Inorg. Chem.* **2010**, *49*, 371−373. (b) Sasamori, T.; Yuasa, A.; Hosoi, Y.; Furukawa, Y.; Tokitoh, N. 1,2-Bis(ferrocenyl)disilene: A Multistep Redox System with an Si=Si Double Bond. *Organometallics* **2008**, *27*, 3325−3327.

(4) (a) Wang, Y. Z.; Xie, Y. M.; Wei, P. R.; King, R. B.; Schaefer, H. F.; Schleyer, P.; Robinson, G. H. A Stable Silicon(0) Compound with a Si=Si Double Bond. *Science* **2008**, *321*, 1069−1071. (b) Ghadwal, R. S.; Roesky, H. W.; Propper, K.; Dittrich, B.; Klein, S.; Frenking, G. A Dimer of Silaisonitrile with Two-Coordinate Silicon Atoms. *Angew. Chem., Int. Ed.* **2011**, *50*, 5374−5378. (c) Yeong, H. X.; Xi, H. W.; Lim, K. H.; So, C. W. Synthesis and Characterization of an Amidinate-Stabilized cis-1,2-Disilylenylethene $[cis\text{-}LSi\{C(Ph)=C\text{-}(H)\}SiL]$ and a Singlet Delocalized Biradicaloid $[LSi(\mu^2\text{-}C_2Ph_2)_2SiL]$. *Chem. − Eur. J.* **2010**, *16*, 12956−12961. (d) Sakya, S. S.; Khan, S.; Nagendran, S.; Roesky, H. W. Interconnected Bis-Silylenes: A New Dimension in Organosilicon Chemistry. *Acc. Chem. Res.* **2012**, *45*, 578−587. (e) Wang, W. Y.; Inoue, S.; Enthaler, S.; Driess, M. Bis(silylenyl)- and Bis(germylenyl)-Substituted Ferrocenes: Synthesis, Structure, and Catalytic Applications of Bidentate Silicon(II)-Cobalt Complexes. *Angew. Chem., Int. Ed.* **2012**, *51*, 6167−6171.

(5) Sen, S. S.; Jana, A.; Roesky, H. W.; Schulzke, C. A Remarkable Base-Stabilized Bis(silylene) with a Silicon(I)-Silicon(I) Bond. *Angew. Chem., Int. Ed.* **2009**, *48*, 8536−8538.

(6) Jones, C.; Bonyhady, S. J.; Holzmann, N.; Frenking, G.; Stasch, A. Preparation, Characterization, and Theoretical Analysis of Group 14 Element(I) Dimers: A Case Study of Magnesium(I) Compounds as Reducing Agents in Inorganic Synthesis. *Inorg. Chem.* **2011**, *50*, 12315−12325.

(7) Gau, D.; Rodriguez, R.; Kato, T.; Saffon-Merceron, N.; de Cozar, A.; Cossio, F. P.; Baceiredo, A. Synthesis of a Stable Disilyne Bisphosphine Adduct and Its Non-Metal-Mediated CO_2 Reduction to CO. *Angew. Chem., Int. Ed.* **2011**, *50*, 1092−1096.

(8) Khoo, S.; Yeong, H. X.; Li, Y. X.; Ganguly, R.; So, C. W. Amidinate-Stabilized Group 9 Metal-Silicon(I) Dimer and -Silylene Complexes. *Inorg. Chem.* **2015**, *54*, 9968−9975.

(9) (a) Khoo, S.; Cao, J.; Ng, F.; So, C. W. Synthesis of a Base-Stabilized Silicon(I)-Iron(II) Complex for Hydroboration of Carbonyl Compounds. *Inorg. Chem.* **2018**, *57*, 12452−12455. (b) Khoo, S.; Cao, J.; Yang, M. C.; Shan, Y. L.; Su, M. D.; So, C. W. Synthesis of a Dimeric Base-Stabilized Cobaltosilylene Complex for Catalytic C-H Bond Functionalization and C-C Bond Formation. *Chem. − Eur. J.* **2018**, *24*, 14329−14334.

(10) He, Z.; Xue, X.; Liu, Y.; Yu, N.; Krogman, J. P. Aminolysis of Bis[bis(trimethylsilyl)amido]-manganese, −iron, and -cobalt for the Synthesis of Mono- and Bis-silylene Complexes. *Dalton Trans.* **2020**, *49*, 12586−12591.

(11) Gütlich, P.; Bill, E.; Trautwein, A. X. *Mössbauer Spectroscopy and Transition Metal Chemistry:Fundamentals and Applications.* Berlin, 2011.

(12) Luecke, M. P.; Porwal, D.; Kostenko, A.; Zhou, Y. P.; Yao, S.; Keck, M.; Limberg, C.; Oestreich, M.; Driess, M. Bis(silylenyl)-substituted Ferrocene-stabilized η^6-Arene Iron(0) Complexes: Synthesis, Structure and Catalytic Application. *Dalton Trans.* **2017**, *46*, 16412−16418.

(13) Blom, B.; Enthaler, S.; Inoue, S.; Irran, E.; Driess, M. Electron-rich N-heterocyclic Silylene (NHSi)-iron Complexes: Synthesis, Structures, and Catalytic Ability of an Isolable Hydridosilylene-iron Complex. *J. Am. Chem. Soc.* **2013**, *135*, 6703−6713.

(14) Blom, B.; Tan, G.; Enthaler, S.; Inoue, S.; Epping, J. D.; Driess, M. Bis-N-heterocyclic Carbene (NHC) Stabilized η^6-Arene Iron(0) Complexes: Synthesis, Structure, Reactivity, and Catalytic Activity. *J. Am. Chem. Soc.* **2013**, *135*, 18108−18120.

(15) (a) Metsänen, T. T.; Gallego, D.; Szilvási, T.; Driess, M.; Oestreich, M. Peripheral Mechanism of a Carbonyl Hydrosilylation Catalysed by an SiNSi Iron Pincer Complex. *Chem. Sci.* **2015**, *6*, 7143−7149. (b) Power, P. P. π-Bonding and the Lone Pair Effect in Multiple Bonds between Heavier Main Group Elements. *Chem. Rev.* **1999**, *99*, 3463−3504.

(16) Ichinohe, M.; Igarashi, M.; Sanuki, K.; Sekiguchi, A. Cyclotrisilenylium ion: The persilaaromatic compound. *J. Am. Chem. Soc.* **2005**, *127*, 9978−9979.

(17) Sarkar, S. K.; Chaliha, R.; Siddiqui, M. M.; Banerjee, S.; Munch, A.; Herbst-Irmer, R.; Stalke, D.; Jemmis, E. D.; Roesky, H. W. A Neutral Three-Membered 2π Aromatic Disilaborirane and the Unique Conversion into a Four-Membered BSi_2N-Ring. *Angew. Chem., Int. Ed.* **2020**, *59*, 23015−23019.

(18) (a) van Lenthe, E.; Baerends, E. J. Optimized Slater-Type Basis Sets for the Elements 1-118. *J. Comput. Chem.* **2003**, *24*, 1142−1156. (b) Becke, A. D. Density-Functional Exchange-Energy Approximation with Correct Asymptotic Behavior. *Phys. Rev. A: Gen. Phys.* **1988**, *38*, 3098−3100. (c) Perdew, J. P.; Yue, W. Accurate and Simple Density Functional for the Electronic Exchange Energy: Generalized Gradient Approximation. *Phys. Rev. B: Condens. Matter* **1986**, *33*, 8800−8802.

(19) Ziegler, T.; Rauk, A. EDA is very informative for Symmetrical Structures with the Orbital Interactions identifiable in Different Irreducible Representations: On the Calculation of Bonding Energies by the Hartree Fock Slater Method. I. The Transition State Method. *Theor. Chim. Acta* **1977**, *46*, 1−10.

(20) (a) von Ragué Schleyer, P.; Kiran, B.; Simion, D. V.; Sorensen, T. S. Does $Cr(CO)_3$ complexation reduce the aromaticity of benzene? *J. Am. Chem. Soc.* **2000**, *122*, 510−513. (b) Cui, Y.-H.; Tian, W.-Q.; Feng, J.-K.; Liu, Z.-Z.; Li, W.-Q. Theoretical studies on the Aromaticity of η^5-Cyclopentadienyl Cobalt Dithiolene Complexes. *J. Mol. Struct.: THEOCHEM* **2007**, *810*, 65−72. (c) Patra, S. G.; Drew, M. G. B.; Datta, D. Delta-Acidity of Benzene in $[(benzene)Ru^{II}(N\text{-}N)Cl]^+$. Crystal Structures, Nuclear Magnetic Resonance Spectra and Nucleus Independent Chemical Shifts. *Inorg. Chim. Acta* **2018**, *471*, 228−233. (d) Jemmis, E. D.; Roy, S.; Burlakov, V. V.; Jiao, H.; Klahn, M.; Hansen, S.; Rosenthal, U. Are Metallocene-Acetylene (M = Ti, Zr, Hf) Complexes Aromatic Metallacyclopropenes? *Organometallics* **2010**, *29*, 76−81.

(21) (a) Stanger, A. Nucleus-Independent Chemical Shifts (NICS): Distance Dependence and Revised Criteria for Aromaticity and Antiaromaticity. *J. Org. Chem.* **2006**, *71*, 883−893. (b) Tsipis, A. C.; Depastas, I. G.; Tsipis, C. A. Diagnosis of the σ-, π- and $(\sigma + \pi)$-Aromaticity by the Shape of the $NICS_{zz}$-Scan Curves and Symmetry-Based Selection Rules. *Symmetry* **2010**, *2*, 284−319.

(22) (a) Landorf, C. W.; Haley, M. M. Recent Advances in Metallabenzene Chemistry. *Angew. Chem., Int. Ed.* **2006**, *45*, 3914−3936. (b) Wadepohl, H.; Castano, M. E. Aromaticity of Benzene in the Facial Coordination Mode: A Structural and Theoretical Study. *Chem. − Eur. J.* **2003**, *9*, 5266−5273.

(23) (a) Bohmann, J. A.; Weinhold, F.; Farrar, T. C. Natural Chemical Shielding Analysis of Nuclear Magnetic Resonance Shielding Tensors from Gauge-including Atomic Orbital Calculations. *J. Chem. Phys.* **1997**, *107*, 1173−1184. (b) Corminboeuf, C.; Heine, T.; Weber, J. Evaluation of Aromaticity: A New Dissected NICS Model based on Canonical Orbitals. *Phys. Chem. Chem. Phys.* **2003**, *5*, 246−251. (c) Heine, T.; von Ragué Schleyer, P.; Corminboeuf, C.; Seifert, G.; Reviakine, R.; Weber, J. Analysis of Aromatic

Delocalization: Individual Molecular Orbital Contributions to Nucleus-Independent Chemical Shifts. *J. Phys. Chem. A* **2003**, *107*, 6470−6475.

(24) Ding, Y.; Sarkar, S. K.; Nazish, M.; Muhammed, S.; Luert, D.; Ruth, P. N.; Legendre, C. M.; Herbst-Irmer, R.; Parameswaran, P.; Stalke, D.; Yang, Z.; Roesky, H. W. Stabilization of Reactive Nitrene by Silylenes without Using a Reducing Metal. *Angew. Chem., Int. Ed.* **2021**, *60*, 27206−27211.

(25) The Jones group recently reported related insertion reactivity of an unligated disilylene toward CO and Fe(CO)₅: Garg, P.; Carpentier, A.; Douair, I.; Dange, D.; Jiang, Y.; Yuvaraj, K.; Maron, L.; Jones, C. Activation of CO Using a 1,2-Disilylene: Facile Synthesis of an Abnormal N-Heterocyclic Silylene. *Angew. Chem.* **2022**, *61*, e202201705.

(26) Sen, S. S.; Tavcar, G.; Roesky, H. W.; Kratzert, D.; Hey, J.; Stalke, D. Synthesis of a Stable Four-Membered Si_2O_2 Ring and a Dimer with Two Four-Membered Si_2O_2 Rings Bridged by Two Oxygen Atoms, with Five-Coordinate Silicon Atoms in Both Ring Systems. *Organometallics* **2010**, *29*, 2343−2347.

(27) Allen, F. H.; Kennard, O.; Watson, D. G.; Brammer, L.; Orpen, A. G.; Taylor, R. Tables of Bond Lengths determined by X-Ray and Neutron Diffraction. Part I. Bond Lengths in Organic Compounds. *J. Chem. Soc., Perkin Trans. 2* **1987**, *2*, S1−S9.

(28) Sen, S. S.; Roesky, H. W.; Stern, D.; Henn, J.; Stalke, D. High Yield Access to Silylene RSiCl (R = PhC(NtBu)2) and Its Reactivity toward Alkyne: Synthesis of Stable Disilacyclobutene. *J. Am. Chem. Soc.* **2010**, *132*, 1123−1126.

(29) Broere, D. L. J.; Coric, I.; Brosnahan, A.; Holland, P. L. Quantitation of the THF Content in Fe[N(SiMe₃)₂]₂·*x*THF. *Inorg. Chem.* **2017**, *56*, 3140−3143.

(30) Dolomanov, O. V.; Bourhis, L. J.; Gildea, R. J.; Howard, J. A. K.; Puschmann, H. OLEX2: a complete structure solution, refinement and analysis program. *J. Appl. Crystallogr.* **2009**, *42*, 339−341.

(31) Sheldrick, G. M. SHELXT − Integrated space-group and crystal-structure determination. *Acta Cryst. A* **2015**, *71*, 3−8.

(32) Sheldrick, G. M. A short history of SHELX. *Acta Crystallogr., Sect. A: Found. Crystallogr.* **2008**, *64*, 112−122.

(33) TURBOMOLE, Version 7.5.1 (TURBOMOLE Gmbh, Karlsruhe, Germany).

(34) ((a)) PQS version 2.4, 2001, *Parallel Quantum Solutions*, Fayetteville, Arkansas, USA (the Baker optimizer is available separately from PQS upon request); (b) Baker, J. An algorithm for the location of transition states. *J. Comput. Chem.* **1986**, *7*, 385−395.

(35) Budzelaar, P. H. M. Geometry optimization using generalized, chemically meaningful constraints. *J. Comput. Chem.* **2007**, *28*, 2226−2236.

(36) (a) Becke, A. D. Density-functional thermochemistry. III. The role of exact exchange. *J. Chem. Phys.* **1993**, *98*, 5648−5652. (b) Lee, C.; Yang, W.; Parr, R. G. Development of the Colle-Salvetti correlation-energy formula into a functional of the electron density. *Phys. Rev. B* **1988**, *37*, 785−789.

(37) (a) Weigend, F.; Ahlrichs, R. Balanced basis sets of split valence, triple zeta valence and quadruple zeta valence quality for H to Rn: Design and assessment of accuracy. *Phys. Chem. Chem. Phys.* **2005**, *7*, 3297−3305. (b) Weigend, F.; Häser, M.; Patzelt, H.; Ahlrichs, R. RI-MP2: optimized auxiliary basis sets and demonstration of efficiency. *Chem. Phys. Lett.* **1998**, *294*, 143−152.

(38) Grimme, S.; Antony, J.; Ehrlich, S.; Krieg, H. A consistent and accurate ab initio parametrization of density functional dispersion correction (DFT-D) for the 94 elements H-Pu. *J. Chem. Phys.* **2010**, *132*, 154104.

(39) (a) von Ragué Schleyer, P.; Maerker, C.; Dransfeld, A.; Jiao, H. J.; van Eikema Hommes, N. J. R. Nucleus-Independent Chemical Shifts: A Simple and Efficient Aromaticity Probe. *J. Am. Chem. Soc.* **1996**, *118*, 6317−6318. (b) von Ragué Schleyer, P.; Manoharan, M.; Wang, Z. X.; Kiran, B.; Jiao, H. J.; Puchta, R.; van Eikema Hommes, N. J. R. Dissected Nucleus-Independent Chemical Shift Analysis of π-Aromaticity and Antiaromaticity. *Org. Lett.* **2001**, *3*, 2465−2468. (c) Chen, Z. F.; Wannere, C. S.; Corminboeuf, C.; Puchta, R.; von Ragué Schleyer, P. Nucleus-Independent Chemical Shifts (NICS) as an Aromaticity Criterion. *Chem. Rev.* **2005**, *105*, 3842−3888.

(40) Gaussian: Gaussian 16, Revision A.03, Frisch, M. J.; Trucks, G. W.; Schlegel, H. B.; Scuseria, G. E.; Robb, M. A.; Cheeseman, J. R.; Scalmani, G.; Barone, V.; Petersson, G. A.; Nakatsuji, H.; Li, X.; Caricato, M.; Marenich, A. V.; Bloino, J.; Janesko, B. G.; Gomperts, R.; Mennucci, B.; Hratchian, H. P.; Ortiz, J. V.; Izmaylov, A. F.; Sonnenberg, J. L.; Williams-Young, D.; Ding, F.; Lipparini, F.; Egidi, F.; Goings, J.; Peng, B.; Petrone, A.; Henderson, T.; Ranasinghe, D.; Zakrzewski, V. G.; Gao, J.; Rega, N.; Zheng, G.; Liang, W.; Hada, M.; Ehara, M.; Toyota, K.; Fukuda, R.; Hasegawa, J.; Ishida, M.; Nakajima, T.; Honda, Y.; Kitao, O.; Nakai, H.; Vreven, T.; Throssell, K.; Montgomery, Jr., J. A.; Peralta, J. E.; Ogliaro, F.; Bearpark, M. J.; Heyd, J. J.; Brothers, E. N.; Kudin, K. N.; Staroverov, V. N.; Keith, T. A.; Kobayashi, R.; Normand, J.; Raghavachari, K.; Rendell, A. P.; Burant, J. C.; Iyengar, S. S.; Tomasi, J.; Cossi, M.; Millam, J. M.; Klene, M.; Adamo, C.; Cammi, R.; Ochterski, J. W.; Martin, R. L.; Morokuma, K.; Farkas, O.; Foresman, J. B.; Fox, D. J. Gaussian, Inc., Wallingford CT, 2016.

(41) (a) McLean, A. D.; Chandler, G. S. Contracted Gaussian basis sets for molecular calculations. I. Second row atoms, Z=11−18. *J. Chem. Phys.* **1980**, *72*, 5639. (b) Krishnan, R.; Binkley, J. S.; Seeger, R.; Pople, J. A. Self-consistent molecular orbital methods. XX. A basis set for correlated wave functions. *J. Chem. Phys.* **1980**, *72*, 650.